Electronic Supplementary Material (ESI) for Biomaterials Science.

Supplemental Materials and Methods

Verification of Epithelial Cell Isolation Purity

Primary ATII cells were isolated and then applied to a cytofunnel (Shandon) at a density of 30,000 cells per 50 µL. Samples were spun onto positively charged glass slides (Hareta) at 600 rpm for 2 minutes. A boundary was drawn around the sample area with a hydrophobic pen (ImmEdge) and samples fixed for 20 minutes at room temperature in 4% paraformaldehyde (in PBS). Samples were then rinsed once with PBS before permeabilization in 0.5% Triton X-100 (in PBS) for 20 minutes at room temperature. Samples were blocked overnight at 4°C in 5% BSA (in PBS). After blocking, samples were incubated in a primary antibody cocktail in 5% BSA for 2 hours at room temperature. Primary antibodies were a directly conjugated AlexaFluor 647 anti-EpCAM (20 µg/mL; BioLegend 118212) and anti-SFTPC (20 µg/mL; ThermoFisher PA571680). Samples were rinsed three times with 0.1% Tween-20 in PBS (PBST) and then incubated in AlexaFluor 488-conjugated secondary antibody (10 µg/mL; ThermoFisher A11034) in 5% BSA for 1 hour. Samples were washed three times in PBST and then incubated in 5 µg/mL Hoechst in PBS. Samples were washed three times with PBS before being mounted under 25 x 75 mm coverslips in Prolong Gold Antifade mounting media (ThermoFisher). Slides were allowed to dry overnight, protected from light, before imaging on an upright epifluorescent microscope. Six 10x images for and three representative 40x images were acquired per slide. Quantification was carried out on the 10x images to maximize the number of cells counted. In Fiji (ImageJ), single

channel images were thresholded, the selection used to create a mask, and clusters of cells in the mask differentiated using the watershed function before particles were counted. An outline overlay of the counted particles was manually compared to the original image to determine if the software had accurately differentiated cells.

Selection of Primary Cell Seeding Densities

Primary ATII cells were isolated and fluorescently labeled by incubation with 10 μM CellTracker™ Green CMFDA Dye (ThermoFisher) in serum-free culture media for 30 min at 37°. Labeled cells were then mixed with hydrogel microspheres at densities of 200, 275, and 350 cells per microsphere (250 microspheres per well). This cell density range was selected based on results from publications that created alveolar cysts using photodegradable hydrogel microspheres, in which 253 primary ATII cells were seeded around each microsphere. A magnetic levitating drive (Greiner BioOne) was placed over the wells and the cells and microspheres were incubated for three days. Each day, images of the same aggregates were taken without removing the levitating drive on an inverted brightfield microscope (Olympus CKX53) using the 4x objective. Cells could be visualized under phase contrast because the incorporated magnetic nanoparticles (NanoShuttle) were visible on each cell. This visualization allowed for qualitative analysis of both cell coverage microsphere packing density over time. After three days, aggregates were sufficiently packed. These structures were then encapsulated in hydrogel as described in the Methods Section and fluorescent images were of the entire structure were obtained using a Keyence BZ-X800 microscope at 4x magnification.

Hydrogel Microsphere Degradation in Response to Exogenous Enzyme

To assess the ability of microspheres to be degraded by exogenous enzyme, discrete regions (~1 cm^2) were drawn on a plain glass slide using a hydrophobic pen (ImmEdge). Microspheres were diluted in serum-free DMEM:F12 to approximately 75 microspheres per 10 µL, and 10 µL of this dilution pipetted to each region on the slide. Elastase (Worthington) was prepared in serum-free DMEM:F12 at stock concentrations of 0.5 and 0.25 mg/mL. Following the acquisition of baseline time 0 images (Olympus, BX-63) 10 µL of enzyme or media alone was pipetted onto microspheres, resulting in final concentrations of 0.25, 0.125, and 0 mg/mL. For the first five minutes, a continuous video was acquired to visualize initial degradation. A static image was then acquired at 5 minutes, followed by a final image after 20 minutes of exposure to enzyme. Static images and single frames from videos were imported to Fiji (ImageJ), and thresholded. The analyze particles function determined the average fluorescence intensity (mean gray value) and number of microspheres per image (n = 15 - 63). Data were presented as percent of initial values.

Hydrogel Microsphere Degradation within 3D Lung Models

Microspheres were generated as described in the Methods Section, but with the incorporation of Methacryloxyethyl Thiocarbamoyl Rhodamine B (Polysciences) to improve microsphere fluorescence over time. Microsphere degradation was analyzed in

response to cell-microsphere interactions within 3D lung models. Aggregates were formed with ATII cells labeled using CellTracker™ Green CMFDA dye and fibroblasts labeled using CellTracker™ Deep Red dye (ThermoFisher). Both dyes were incubated with cells at a 10 μM concentration in serum-free cell culture media for 30 min at 37°. One day after embedding, and weekly up to three weeks, aggregates were imaged live on an upright, epifluorescence microscope (Olympus, BX-63). A single z-stack (200 μm thick; 10 μm step size; 10x magnification) was taken within the middle of each aggregate. This image size was sufficient to capture nearly the entire structure. New aggregates were imaged at the same exposure setting at each time point to exclude the influence of photobleaching on the results. Spectral overlap of the deep red dye into the red channel used to capture rhodamine fluorescence was observed, however, this did not influence microsphere evaluation. Maximum projections of each channel were generated from the z-stack, and then in Fiji (ImageJ) the image calculator function subtracted the deep red spectral overlap from the red microsphere images, leaving an image of only microspheres. This image was thresholded and the mean gray value measured and recorded as average microsphere intensity per aggregate.

TGFβ ELSIA

Following live/dead imaging, individual 3D lung models containing both fibroblasts and epithelial cells in either soft or stiff embedding hydrogels were incubated in 100 μL of 2 mg/mL collagenase B (Roche) for 30 min at 37°. Digested material was vortexed and then spun briefly to pellet any remaining debris. Levels of TGFβ in these hydrogel extracts

were assayed using a TGF-beta 1 Quantikine ELISA kit (R&D systems). Samples were activated with 1M HCL, quenched with 1.2M NaOH in HEPES, and then sequentially incubated alongside a standard curve in pre-coated ELISA wells with assay diluent, TGFβ conjugate, and substrate solution. The colorimetric assay was halted with stop solution and absorbance read on a BioTek Synergy H1 plate reader at 450nm (with a separate reading at 570 nm for background subtraction. Concentrations wee interpolated from the standard curve in GraphPad Prism 9.

Supplemental Results

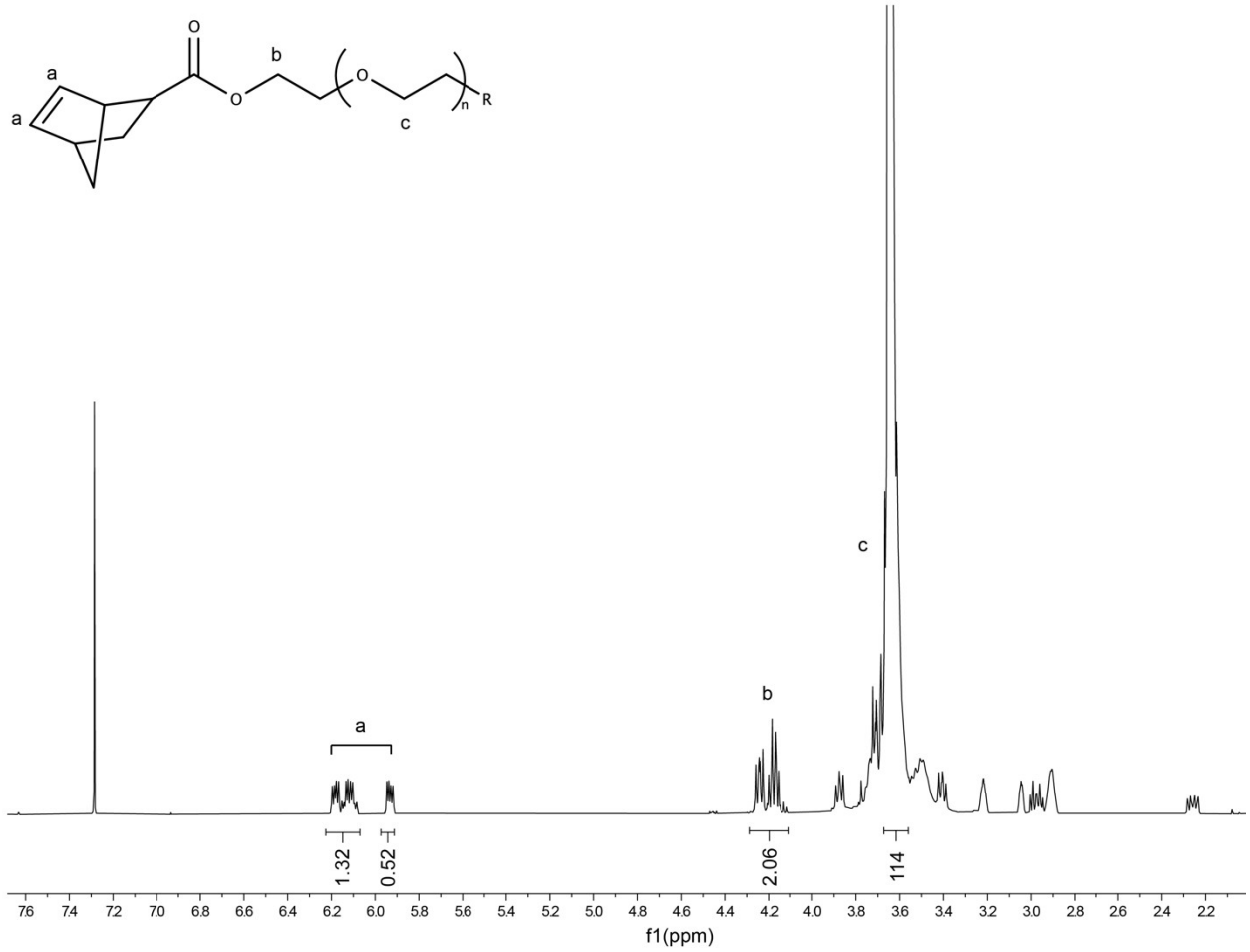

Figure S1. ^{1}H NMR of 10 kg/mol poly(ethylene glycol) norbornene (PEGNB). δH (ppm) (300 MHz, $CDCl_3$, Me_4Si): 3.71 (s, 114H, PEG CH_2-CH_2), 4.1-4.2 (m, 2H, -CH_2-O), 5.9-6.2 (m, 2H, –CH=CH-). NMR shows quantitative norbornene functionalization based on a comparison of the alkene protons from norbornene to the theoretically expected number of alkene protons, using the ethylene glycol protons as a reference. Functionalization was measured as 92%.

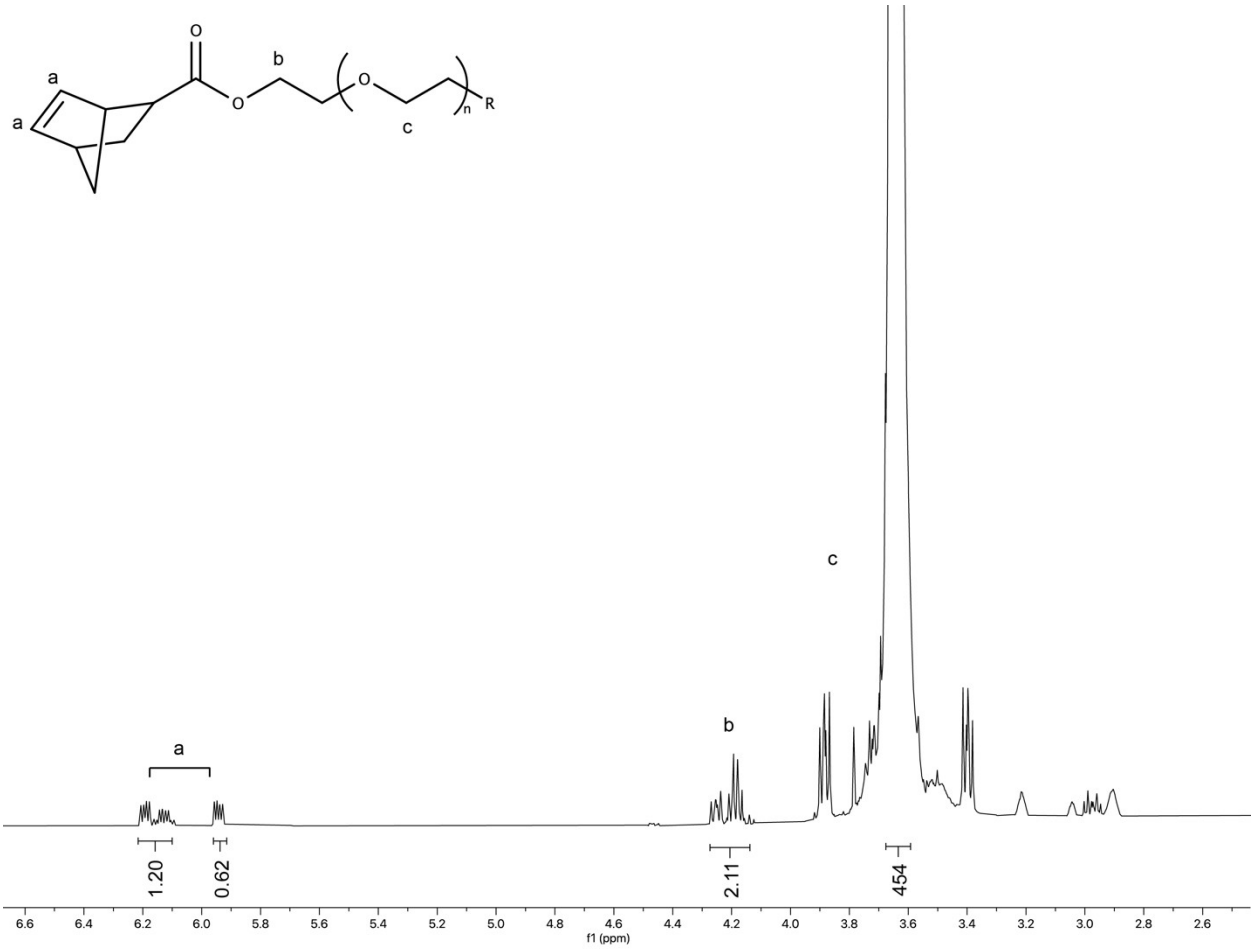

Figure S2. ^{1}H NMR of 40 kg/mol poly(ethylene glycol) norbornene (PEGNB). δH (ppm) (300 MHz, $CDCl_3$, Me_4Si): 3.71 (s, 114H, PEG CH_2-CH_2), 4.1-4.2 (m, 2H, -CH_2-O), 5.9-6.2 (m, 2H, –CH=CH-). NMR shows quantitative norbornene functionalization based on a comparison of the alkene protons from norbornene to the theoretically expected number of alkene protons, using the ethylene glycol protons as a reference. Functionalization was measured as 91%.

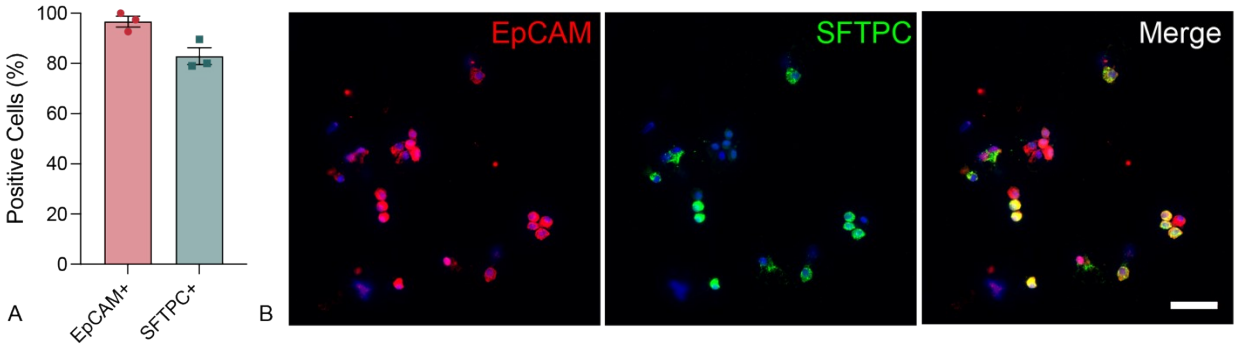

Figure S3. Immunocytochemistry revealed high purity of ATII cells following magnetic column isolation. A) Quantification of staining results demonstrated that the isolation procedure gave 96.7 ± 2.1% EpCAM+ (epithelial) cells and 82.9 ± 3.4% SFTPC+ (ATII) cells. N = 3 independent isolations. B) Representative images showed staining for EpCAM (red) and SFTPC (green) consistent with the measured values. Scale bars, 50 µm.

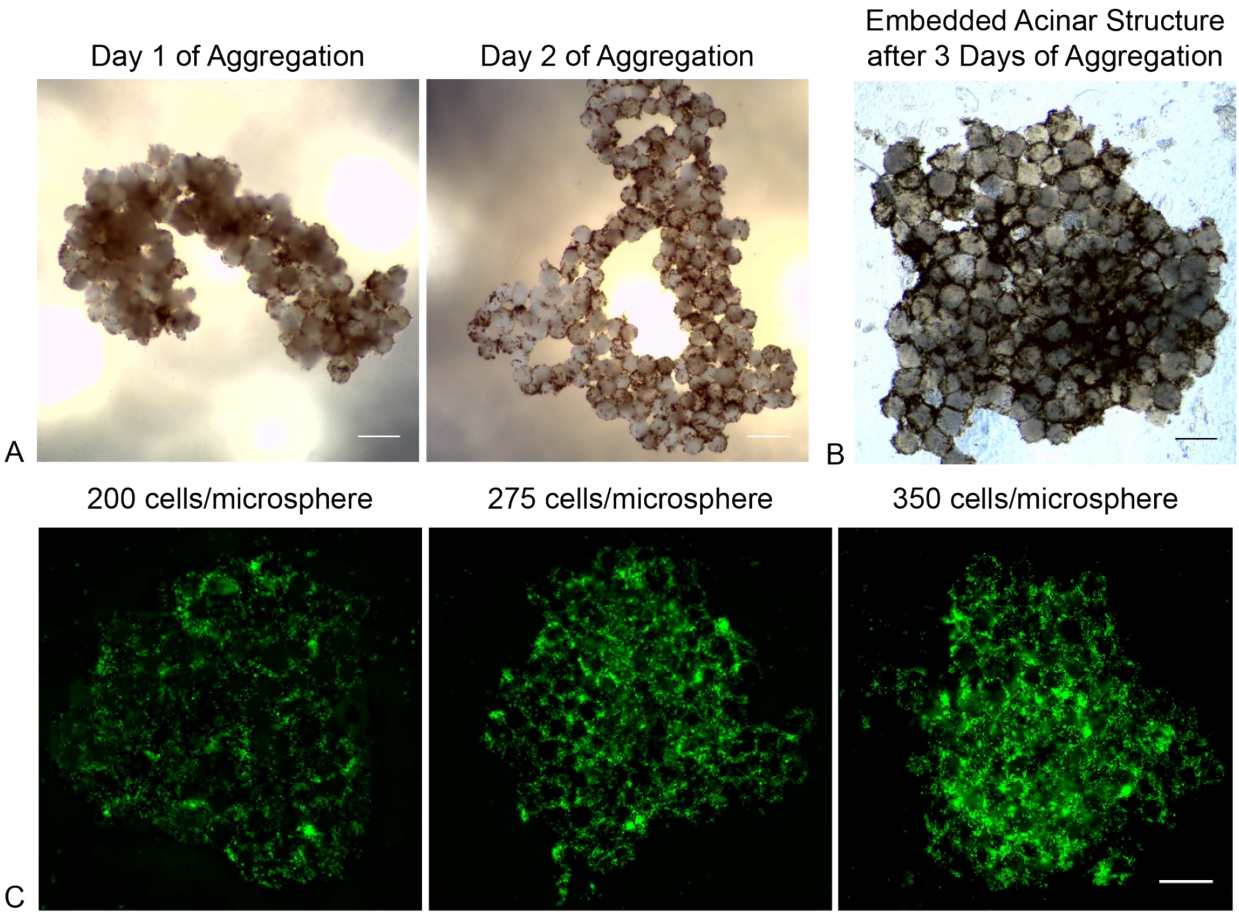

Figure S4. Adjustment of aggregation time and ATII seeding density. A) Phase contrast images acquired on an inverted microscope with the magnetic drive still present above the wells. Both one- and two-days post-seeding aggregate structure was coalescing but irregular. B) Phase contrast image acquired on day three post-embedding, without the presence of the magnetic drive. The overall aggregate structures post-embedding were tightly packed, 200 - 400 μm (one to two microspheres) thick, and 2-2.5 mm in diameter. C) Fluorescent images of ATII cells labeled with CellTracker Green and seeded at different densities relative to total microspheres. 200 cells per microsphere resulted in

incomplete cell coverage whereas 350 cells per microsphere created barriers thicker than a single cell between microspheres. Scale bars, 500 μm.

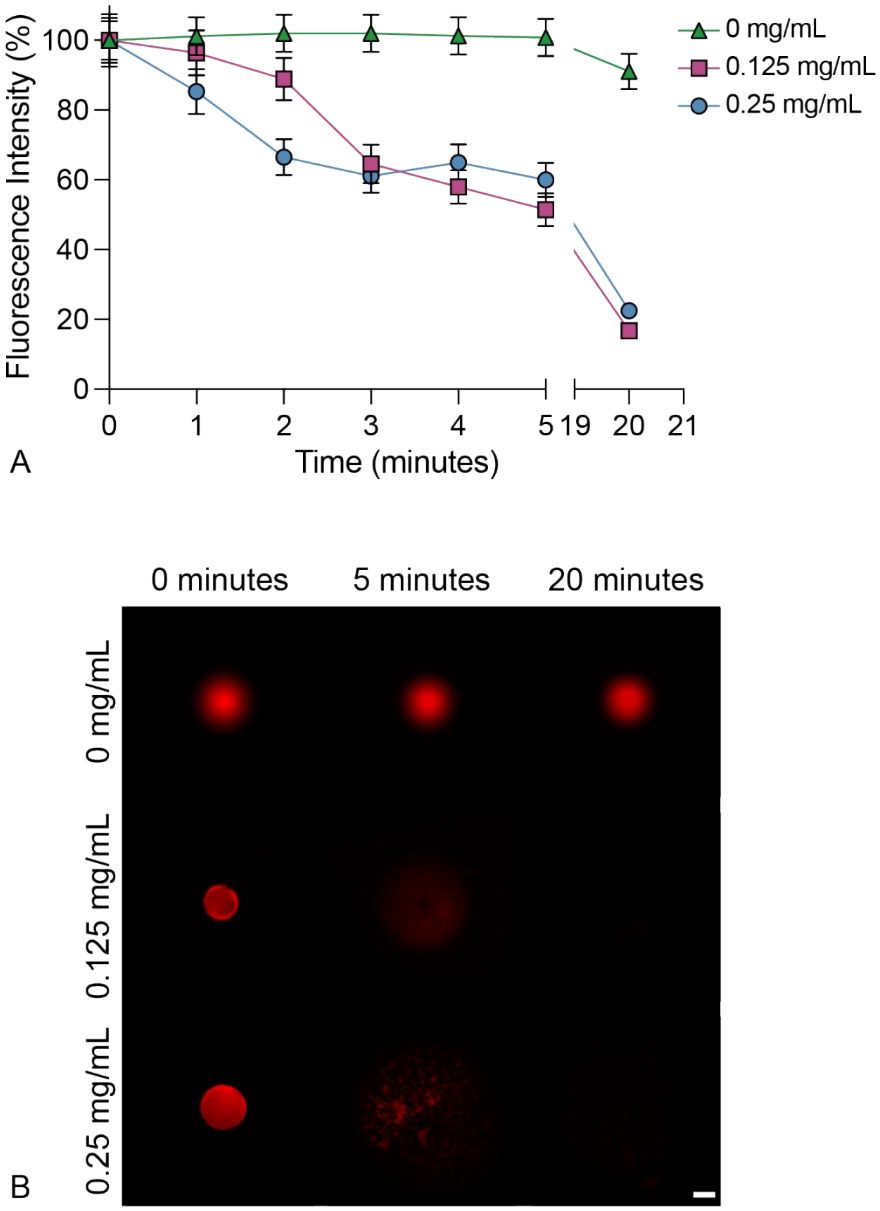

Figure S5. Enzymatic degradation of hydrogel microspheres. A) Rhodamine-labeled microspheres were exposed to elastase and imaged at time points up to 20 minutes.

Fluorescent intensity of the microspheres was quantified in Fiji (ImageJ; n = 15-63 microspheres. Scale bar, 50 μm. B) Representative images show rapid degradation of spheres by exogenous elastase, occurring as early as 5 minutes with almost complete degradation by 20 minutes.

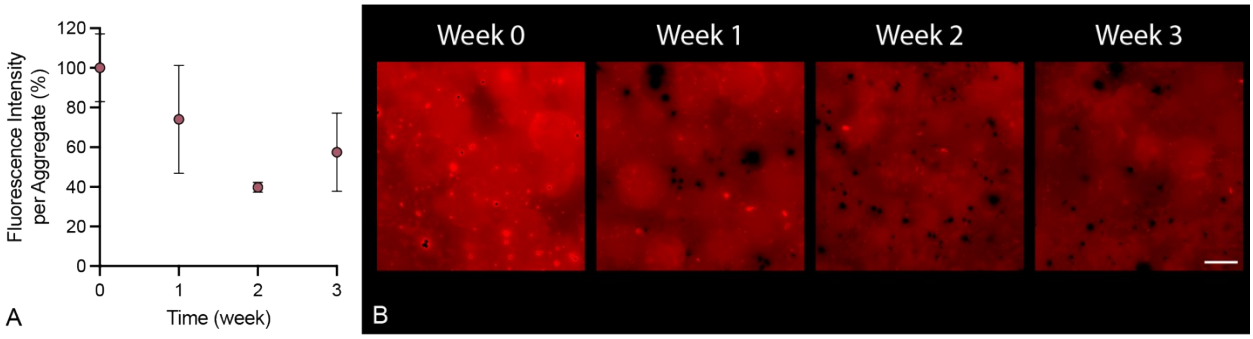

Figure S6. Degradation of hydrogel microspheres within 3D lung models. A) Quantification of microsphere fluorescent intensity over time within cell-laden embedded aggregates. Data are presented as percent of starting fluorescence (n = 5-7 aggregates per time point; Scale bar, 100 μm). B) Representative images show partial, but not complete, degradation of the microspheres by endogenous cellular enzyme secretion.

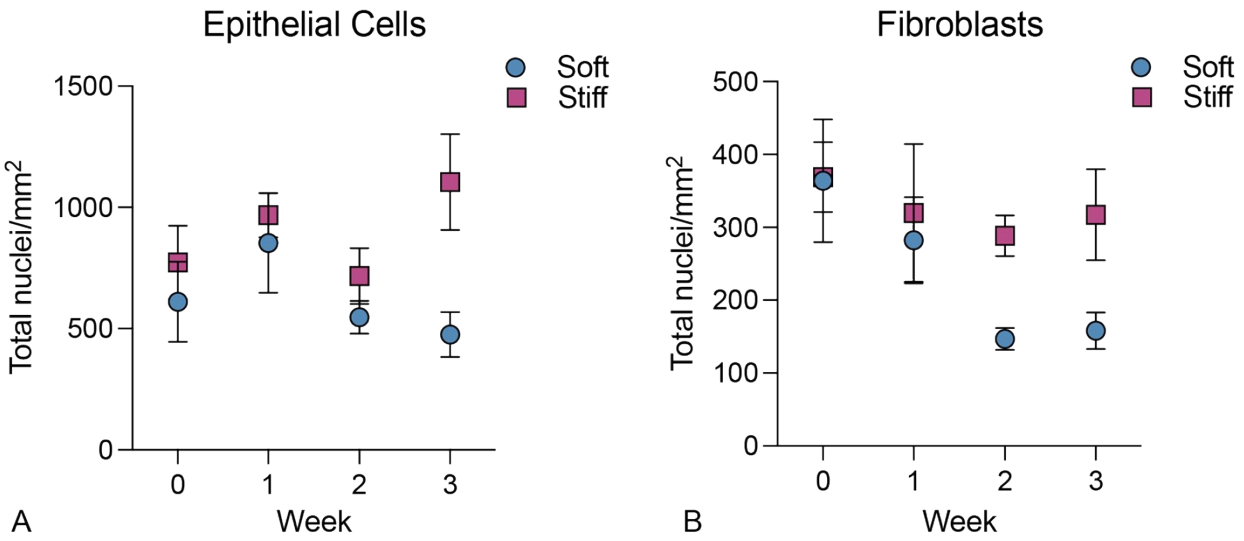

Figure S7. Total number of A) epithelial cells and B) fibroblasts per area, quantified from live/dead staining images. Numbers of epithelial cells remained largely stable, with an increase at Week 3 in the stiff microenvironment only, which could be suggestive of delayed proliferation. Fibroblast populations showed a non-significant decrease, more notably in the soft hydrogel microenvironment, while fibroblasts in the stiff microenvironment may have been able to proliferate enough to better maintain overall numbers (n=5-7). There were no statistical differences between soft and stiff or among time points (two-way ANOVA).

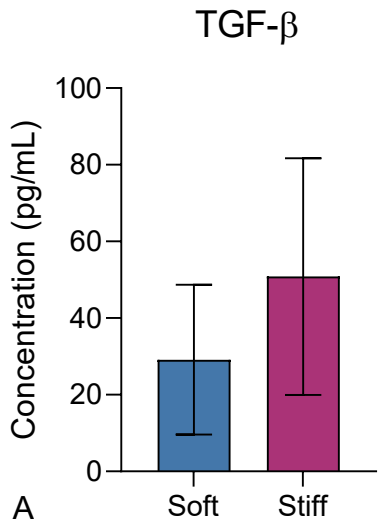

Figure S8. Results of an ELISA for TGFβ secreted by cells within the 3D lung models showed a trend towards increased TGFβ in stiff microenvironments with no measurable statistical differences (n=3; t-test).

Table S1. Results of the Qiagen RT^2 fibrosis array. Nine aggregates per condition were generated and RNA extracted from three sets of three pooled aggregates. Gene expression of these three samples per condition was normalized to the housekeeping gene beta-2 microglobulin (B2M) and is presented as 2^(Average ΔC_T). Genes with a fold change of greater than 2 (either up- or down-regulated) were grouped into families based on general function and incorporated into the heatmap presented in Figure 6.

	FIBROBLASTS ONLY		FIBROBLAST-EPITHELIAL CELL CO-CULTURE	
GENE	**Soft**	**Stiff**	**Soft**	**Stiff**
ACTA2	0.023115	0.046100	0.152077	0.403288
AGT	0.142389	0.010813	0.076587	0.009852
AKT1	0.017211	0.066068	0.020100	0.156426
BCL2	0.056153	0.019498	0.271377	0.065868
BMP7	0.042645	0.040496	0.042298	0.022908
CAV1	0.006946	0.010813	0.009197	0.037515
CCL11	0.642826	0.500234	0.605843	1.032620
CCL12	0.008961	0.010813	0.009197	0.005624
CCL3	0.091166	0.136187	0.387746	0.069958
CCR2	0.224224	2.199090	0.350301	0.573006
CEBPB	0.027454	0.104752	0.094385	0.063284
COL1A2	0.057691	1.267547	0.038948	5.538648
COL3A1	0.007843	0.077335	0.010056	0.005624
CCN2	0.537860	5.798895	1.811276	4.168111
CXCR4	0.025908	0.020874	0.019581	0.008072
DCN	0.006946	0.010813	0.009197	0.052643
EDN1	0.017375	0.012949	0.009197	0.005624
EGF	0.028287	0.090310	0.058559	0.059618
ENG	2.180932	1.012330	4.139187	0.965942
FASL	0.006946	0.010813	0.009197	0.005624
GREM1	1.733553	0.909331	2.167326	1.137279
HGF	0.012931	0.017879	0.026314	0.005624
IFNG	0.006946	0.010813	0.009197	0.005624
IL10	0.006946	0.010813	0.010517	0.005624
IL13	0.006946	0.014438	0.009197	0.048088

IL13RA2	0.006946	0.016470	0.009197	0.005624
IL1A	0.245278	0.044780	0.304143	0.056882
IL1B	1546.584661	0.012342	0.009197	0.005624
IL4	0.084895	0.015532	0.012582	0.008229
IL5	0.567125	0.357914	0.097307	0.072506
ILK	523.092594	0.016440	1501.100288	0.009188
INHBE	0.043322	0.014178	0.165460	0.021226
ITGA1	0.006946	0.010813	0.009197	0.042963
ITGA2	0.040001	0.010813	0.026428	0.005624
ITGA3	1.166827	3.397777	2.442170	0.806789
ITGAV	0.016095	0.050901	0.025148	0.060547
ITGB1	0.341361	2.241692	1.018529	0.702205
ITGB3	0.220681	0.249041	0.103623	0.167278
ITGB5	0.021492	1.013785	0.065217	0.091544
ITGB6	3.271760	2.518972	3.080787	1.605086
ITGB8	0.006946	0.010813	0.009197	0.005624
JUN	0.037147	0.078617	0.114391	0.061485
LOX	0.235155	0.119576	0.225299	0.135057
LTBP1	4.641140	3.371719	6.919539	1.823036
MMP13	0.066071	0.103490	0.065388	0.072571
MMP14	0.093480	0.042719	0.369381	0.051176
MMP1A	0.098361	0.041945	0.079240	0.043583
MMP2	0.010786	0.612496	0.018758	0.005624
MMP3	0.012194	0.241960	0.017803	0.008841
MMP8	0.006946	0.035123	0.012470	0.058587
MMP9	19.164840	24.343119	9.612396	7.366333
MYC	0.010828	0.015233	0.023334	0.088948
NFKB1	0.006946	0.010813	0.044423	0.005624
PDGFA	0.041027	0.184409	0.175842	0.020221
PDGFB	0.428825	0.196830	1.338988	0.509543
PLAT	0.008315	0.010813	0.041455	0.005624
PLAU	0.013390	0.010813	0.009197	1.160750
PLG	0.006946	0.014136	0.009197	0.005624
SERPINA1A	0.006946	0.010813	0.009452	0.005624
SERPINE1	0.015728	0.090494	0.065855	0.053102
SERPINH1	0.600204	0.680867	1.196838	0.469785
SMAD2	0.049775	0.062378	0.069916	0.008672
SMAD3	0.024958	0.105449	0.165764	0.016647
SMAD4	0.009186	0.010813	0.009197	0.005624

SMAD6	0.014948	0.016674	0.075506	0.005624
SMAD7	0.017945	0.010813	0.013652	0.005805
SNAI1	4.312381	2.434878	12.567139	1.866353
SP1	0.006946	0.010813	0.009197	0.042891
STAT1	0.009586	0.010813	0.009197	0.060121
STAT6	0.013398	0.010813	0.021882	0.005624
TGFB1	0.013113	0.101349	0.175266	0.032165
TGFB2	0.008760	0.010813	0.009197	0.005624
TGFB3	0.107789	0.115890	0.158928	0.076301
TGFBR1	1421.213798	562.434211	0.040151	2470.530030
TGFBR2	0.080413	1.584059	0.149572	0.068948
TGIF1	0.006946	0.010813	0.009197	0.005624
THBS1	2.040383	5.007967	3.081836	6.023597
THBS2	0.030309	0.010813	0.009197	0.005624
TIMP1	0.515227	0.469993	1.277961	0.710572
TIMP2	0.051357	0.084221	3.607032	0.430524
TIMP3	0.021893	0.010813	0.009197	0.095427
TIMP4	0.075947	0.022248	0.148735	0.049860
TNF	0.014926	0.013811	0.033036	0.005624
VEGFA	0.021634	0.082852	0.023748	0.051422
ACTB	0.151423	4.261739	0.172660	7.719022
B2M	1.000000	1.000000	1.000000	1.000000
GAPDH	0.065652	1.901670	0.238814	0.532098
GUSB	0.207064	0.054150	0.113791	0.017147
HSP90AB1	3.385784	1.304292	3.142099	2.543036